AIP | Applied Physics Letters

Voltage tuning of plasmonic absorbers by indium tin oxide

Fei Yi, Euijae Shim, Alexander Y. Zhu, Hai Zhu, Jason C Reed et al.

Citation: Appl. Phys. Lett. **102**, 221102 (2013); doi: 10.1063/1.4809516
View online: http://dx.doi.org/10.1063/1.4809516
View Table of Contents: http://apl.aip.org/resource/1/APPLAB/v102/i22
Published by the AIP Publishing LLC.

Voltage tuning of plasmonic absorbers by indium tin oxide

Fei Yi, Euijae Shim, Alexander Y. Zhu, Hai Zhu, Jason C Reed, and Ertugrul Cubukcu[a)]
Department of Materials Science and Engineering, University of Pennsylvania, 3231 Walnut St., Philadelphia, Pennsylvania 19104, USA

(Received 11 April 2013; accepted 17 May 2013; published online 3 June 2013)

We experimentally demonstrate electrical tuning of plasmonic mid-infrared absorber resonances at 4 μm wavelength. The perfect infrared absorption is realized by an array of gold nanostrip antennas separated from a back reflector by a thin dielectric layer. An indium tin oxide active layer strongly coupled to the optical near field of the plasmonic absorber allows for spectral tunability. © *2013 AIP Publishing LLC*. [http://dx.doi.org/10.1063/1.4809516]

Metallic nanostructures support localized surface plasmons that can be excited resonantly by suitably matching the excitation wavelength to the size of the plasmonic resonator. On resonance, plasmonic nanoantennas can localize the freely propagating radiation and produce very high optical currents in the metal.[1] Due to the free electron absorption in metals, electromagnetic energy is efficiently converted to heat similar to generation of heat in a resistor at radio frequencies. Various types of resonant plasmonic absorbers utilizing this effect have been demonstrated for radiation absorption across the electromagnetic spectrum.[2–4] The electrical tunability of a plasmonic absorber that enables electro-optical switching is highly desirable, however, has not been achieved previously. Recently, it has been reported that significant voltage-tunable changes in the refractive index of indium tin oxide (ITO) can be achieved through accumulation of carriers through the electric field effect when utilizing ITO in a metal-oxide-semiconductor capacitor configuration.[5–7] In this work, we demonstrate an electrically tunable plasmonic absorber with near unity absorption enabled by ITO as the active material.

The schematic of the electrically tunable plasmonic absorber is shown in Fig. 1. Periodic gold nanostrips are fabricated on top of a free standing silicon nitride membrane with a silicon frame using standard electron beam lithography and lift-off processes. The backside of the nitride membrane spacer is coated with a 100 nm thick gold layer, acting simultaneously as the back electrode and the back reflector allowing for near unity absorption in the plasmonic absorber design first proposed by Shvets *et al.*[3] The gold nanostrips and back plate also act as the top and bottom contact electrodes for carrier injection and electrostatic gating, respectively. For electrical tunability, a thin layer of ITO is then deposited directly on the nanostrip antennas, where the near field intensity is maximum. Figure 1 also shows the scanning electron microscope (SEM) image of the fabricated nanostrip plasmonic absorber.

The carriers injected into the ITO create an accumulation layer and modulate the optical refractive index in the near field of the plasmonic absorber, which in turn leads to the tuning of the plasmonic absorption resonance.[5,6]

We first numerically analyze the two-dimensional periodic absorber structure using an electromagnetic solver (COMSOL). Figure 2(a) shows the schematic diagram of a unit cell of the studied periodic structure. We find that the spectral position of the peak absorption depends predominantly on the width (W_g) of the nanostrips, since the nanostrips act as resonators for light polarized along their width. The absorption efficiency can be maximized for an optimal filling factor, $F \equiv W_g/D$, defined by the ratio between W_g and the array period D. For each W_g, there is an optimal period for the resonant absorption to reach unity. For example, for $W_g = 200$ nm, the peak absorption approaches unity at $\lambda_{plasmon} = 2\,\mu$m corresponding to $F_{opt} = 0.14$, while $F_{opt} = 0.67$ for $D = 1000$ nm, $\lambda_{plasmon} = 5.7\,\mu$m. For a certain W_g, if the filling factor F is not at its optimal value, then peak absorption will deviate from unity. As shown in Fig. 2(d), for $W_g = 600$ nm, when filling factor F is decreased from the optimal value of $F = 0.33$ ($D = 1800$ nm) to $F = 0.2$ ($D = 3000$ nm), the peak absorption is moderately reduced from unity to about 90%. From the numerical simulations, we can see that unity absorption can be sustained even for resonance wavelengths up to 6 μm and peak absorption monotonically decreases above 6 μm. In the wavelength range for which unity absorption can be achieved, the ratio of plasmonic resonant wavelength, $\lambda_{plasmon}$, to the thickness, t, of the dielectric spacer is $\eta_{plasmon} \equiv \lambda_{plasmon}/t = 60$.

Note that this corresponds to a much thinner spacer layer compared to that in a conventional absorber based on wave interference, where the wavelength of the first absorption peak appears at $\lambda_{abs} = 4n_{nitride}t \sim 8t$, only 8 times the thickness of the nitride spacer.[3,4,8] Therefore, the unique advantage of such "nanostrip antenna/dielectric spacer/back mirror" structure is that optically it can support plasmonic resonances with a spacer thickness that is 60 times smaller than the resonant wavelength,[3] which is crucial for tuning the optical spectra with a low applied gate voltage.

To demonstrate the electrical tuning of the absorption spectrum, an ITO layer of ~15 nm is deposited on top of the gold nanostrip antennas and the nitride spacer, as shown in Fig. 3(a). An identical ITO layer deposited on a silicon sample during the same sputtering process is used for optical characterization. The refractive index, n, and the extinction coefficient, κ, of the ITO films measured by a spectroscopic ellipsometer are shown in Fig. 3(b). We fitted our ellipsometry data using the Drude model:[5,6]

[a)]Author to whom correspondence should be addressed. Electronic mail: cubukcu@seas.upenn.edu

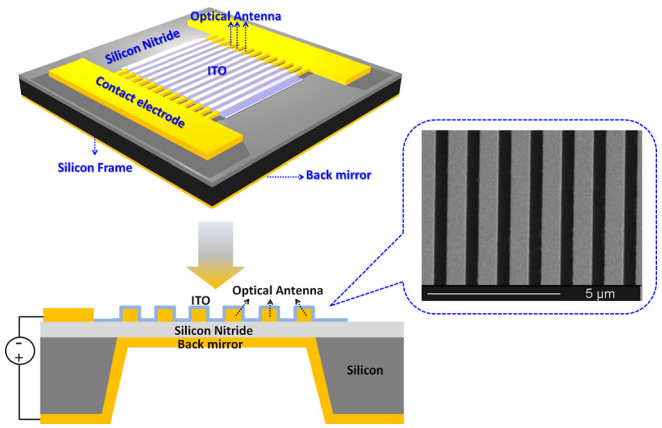

FIG. 1. A schematic overview of the electrically tunable optical antenna absorber. Plasmonic nanostrip antennas fabricated on a silicon nitride membrane with a gold back reflector. A thin layer of ITO deposited on the nanostrips acts as the active layer for electrical tuning. The gold nanostrips and the gold back mirror are also used as the contact electrodes for carrier injection into the ITO layer. Inset: an SEM image of a typical absorber.

$$\varepsilon = \varepsilon_\infty - \frac{\omega_p^2}{\omega^2 + i\omega\gamma}. \tag{1}$$

The following fitting parameters produced the best fit to our index of refraction data; background permittivity $\varepsilon_\infty = 2.17$, collision frequency $\gamma = 190$ THz, plasma frequency $\omega_p = 8.75 \times 10^{14}$ rad s^{-1}. From the plasma frequency, ω_p, we extracted the initial carrier concentration, n_c, of the deposited ITO film: $n_c = \varepsilon_0 m^* \omega_p^2 / e^2$, where $m^* = 0.35 \times m_0$ is the effective mass of electrons in ITO and m_0 is the electron rest mass, e is the electron charge, and ε_0 is the vacuum permittivity. The initial electron concentration n_c is found to be 8.8×10^{19} cm^{-3}.

We fabricated an array of nanostrip antennas using electron beam lithography on a 100 nm thick silicon nitride membrane with 100 nm of gold back mirror evaporated on the back side.

Then, 15 nm of ITO is sputtered as the active material on the nanoantennas. A current source meter (Keithley 2400) applied a voltage across the ITO/nitride spacer to inject carriers into the ITO layer. Figure 3(c) shows the leakage current, I_g, through the dielectric spacer as a function of applied bias voltage. It can be seen that the capacitor structure can sustain an applied voltage, V_g, up to 20 V without dielectric breakdown. This value (20 V/100 nm) is close to the typical breakdown voltages of silicon nitride thin films.[9] We measured the absorption spectrum of the plasmonic absorbers under different applied bias voltages using a Fourier transform infrared spectrometer (FTIR) coupled to an infrared microscope equipped with reflective optics. Figure 3(d) shows that the absorption spectrum is tuned by the modulated refractive index in the near field region of the plasmonic absorber where the injected carriers accumulated. For an applied voltage of 10 V, a shift of ~10 nm in the absorption spectrum is experimentally demonstrated (Fig. 3(d)).

In order to reproduce the experimentally obtained results, we need to determine the carrier concentration in the accumulation layer. The average thickness t_a of the accumulation layer created by the carriers injected into the ITO layer in a standard metal-insulator-semiconductor structure as shown in Fig. 4(a) is given by[10]

$$t_a = \frac{\pi}{\sqrt{2}} \sqrt{\frac{k_B T \varepsilon_0 \varepsilon_s}{n_c q^2}}. \tag{2}$$

Here, k_B is the Boltzmann constant; $T = 300$ K is the absolute temperature; q is the electron charge; ε_0 is the free space permittivity, and $\varepsilon_s = 9.3$ is the relative static permittivity of ITO. Using the aforementioned $n_c = 8.8 \times 10^{19}$/cm^3, the thickness of the accumulation layer is found to be $t_a = 0.9$ nm. To verify the value of t_a obtained by Eq. (2), we also used a 2D simulation package[11] to find the distribution of the injected carriers in the ITO and the result is shown in

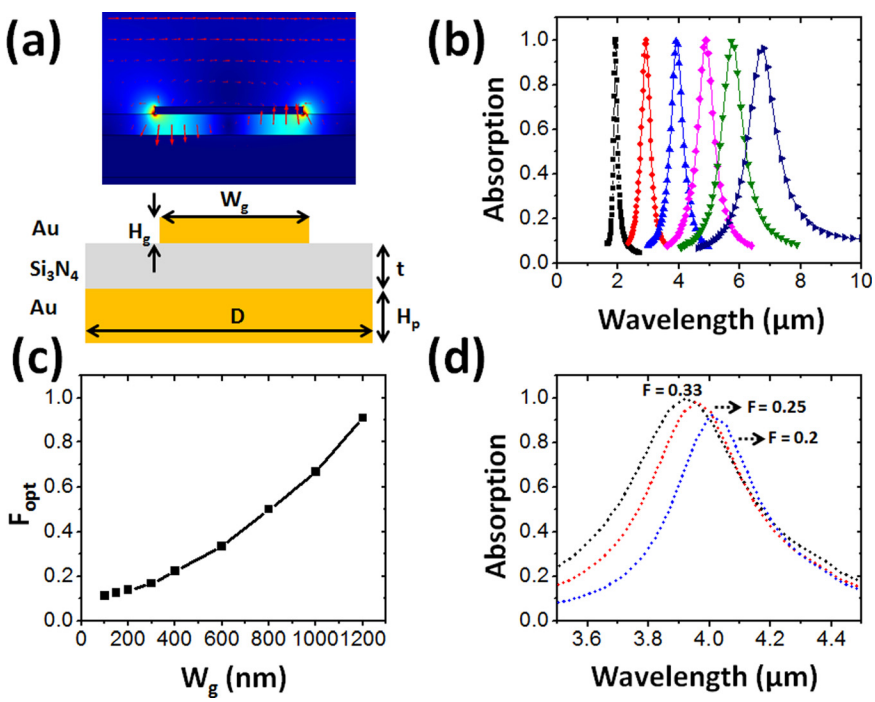

FIG. 2. (a) Schematic of the plasmonic absorber. (Top) Optical near field distribution for a unit cell. The dimensions in our devices are: $t = 100$ nm, $H_g = 35$ nm, and $H_p = 200$ nm. (b) The optimal optical spectra of nanostrip antenna with W_g of 200 nm (■), 400 nm (●), 600 nm (▲), 800 nm (◆), 1000 nm (▼), and 1200 nm (▶). (c) The corresponding optimal filling factor F_{opt} for each W_g. (d) The optical spectra for $W_g = 600$ nm with different filling factors.

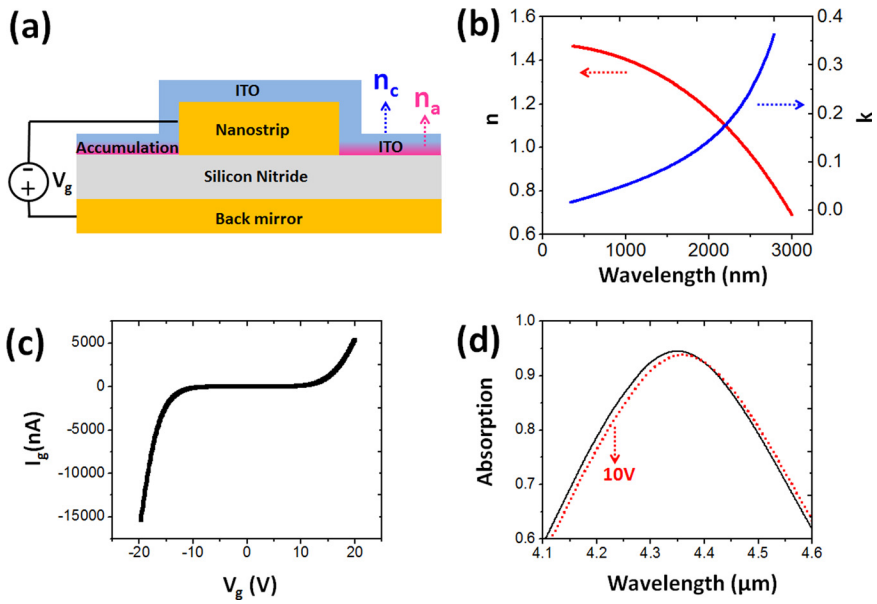

FIG. 3. (a) A thin layer of ITO is placed at the optical near field region of the plasmonic nanostrip antenna. Electrically a capacitor structure is formed with the silicon nitride as the dielectric spacer. An accumulation layer builds up in the ITO at the ITO/silicon nitride interface. The carrier concentration at the accumulation layer, n_a, is higher than that of the initial ITO film n_c. (b) The refractive index n and extinction coefficient κ of the as deposited ITO layer measured by ellipsometry. (c) The leakage current for the "ITO/dielectric spacer/gold backplate" structure under applied bias. (d) The tuning of the measured absorption spectra by carriers injected into the ITO layer.

Fig. 4(b). It can be seen that under 10 V of gate voltage, the carrier concentration is $1.45 \times 10^{20}/\text{cm}^3$ at the ITO/silicon nitride interface and then drops exponentially to the intrinsic carrier concentration of $8.8 \times 10^{19}/\text{cm}^3$ after about 1.5 nm in good agreement with the value from Eq. (2). Having calculated t_a, we can find the injected carrier concentration n_{acc} in the accumulation layer. The total injected charge Q of the capacitor is $Q = C_i \times V_g = V_g \times \varepsilon_0 \times \varepsilon_i \times A/t$, where A is the unit area of the capacitor and $t = 100$ nm is the thickness of the silicon nitride spacer. $\varepsilon_i = 4$ is the static relative permittivity of silicon nitride.[5] Assuming a uniform carrier distribution in the accumulation layer, the injected carrier concentration can, therefore, be calculated as

$$n_{acc} = \frac{Q/e}{A \times t_a} = \frac{\varepsilon_i \varepsilon_0 V_g}{t \times t_a \times e}. \tag{3}$$

Under an applied voltage of $V_g = 10$ V, the injected carrier concentration in the accumulation layer n_{acc} is found to be $2.2 \times 10^{19}\,\text{cm}^{-3}$ corresponding to a total carrier concentration ($n_a = n_c + n_{acc}$) of $1.1 \times 10^{20}\,\text{cm}^{-3}$. Although we underestimate the carrier density assuming a uniform distribution, this agrees well with average carrier density in the accumulation layer from the electrical simulations.

Using the estimated carrier concentration, we determined the changes in the real and imaginary parts of the dielectric constant for ITO (Fig. 4(c)). We can see that the dielectric constants in the accumulation region are changed by the injected carriers at longer wavelengths. We calculated, by solving the 3D problem in COMSOL, the absorption spectrum of the plasmonic absorber covered with the ITO layer by inputting the calculated dielectric constant after carrier accumulation under 10 V bias. The accumulation layer is modeled as a 1 nm thick layer at the ITO/nitride interface with a uniform carrier concentration. The accumulation layer lies within the strongest region of the plasmonic mode. The absorption spectra before and after the carriers are injected into the ITO layer are shown in Fig. 4(d). The simulated

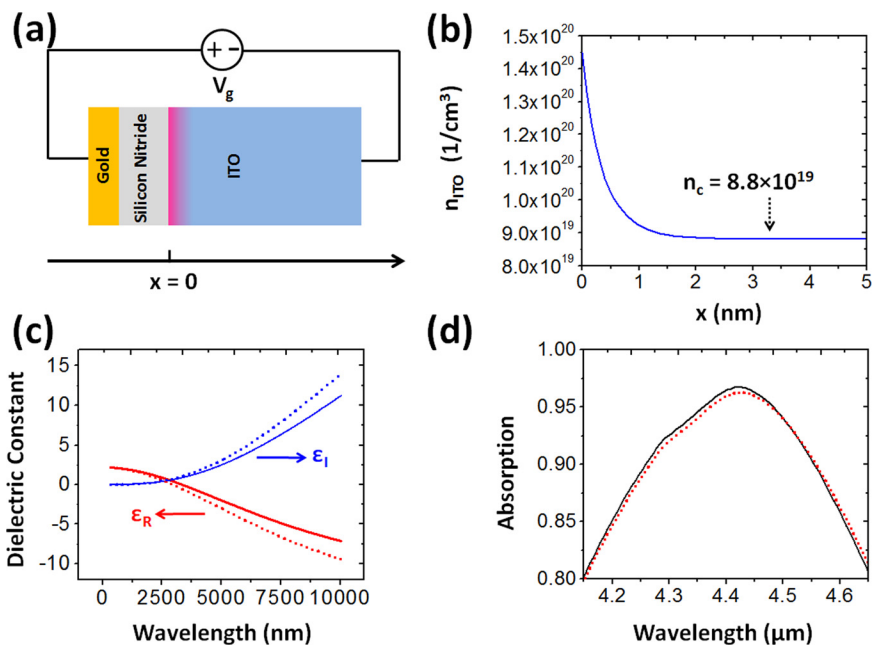

FIG. 4. (a) The "metal-insulator-semiconductor" capacitor structure used to calculate the injected electron density in the ITO accumulation layer. (b) The simulated distribution of the electron density in the ITO layer. Here, x is the distance from the ITO/nitride interface. (c) The real (red) and imaginary (blue) parts of the dielectric constant in the accumulation region before (solid lines) and after (dotted lines) carrier injection by applied bias voltage. (d) Numerical simulation of the absorption spectrum tuning caused by the accumulation layer of the injected carriers. The black solid line is the absorption spectrum without injected carriers, while the red dotted line is the absorption spectrum with injected carriers.

spectral shift of around 8 nm agrees well with the measured value.

The amount of spectral tuning strongly depends on the injected carrier concentration in the accumulation layer, which is limited by the breakdown field for the dielectric spacer used, similar to gate oxide breakdown in metal-oxide-semiconductor field effect transistors (MOSFETs). With typical electrical breakdown fields, our calculations and experiments show that the upper limit for injected carrier density (n_{acc}) is in the $10^{19}\,cm^{-3}$ range. For our initial carrier concentration, this corresponds to a change of only 20%. Since the upper limit for the injected carrier density is determined by the dielectric breakdown, it is not possible to achieve higher injected carrier density by utilizing a thinner dielectric spacer. Although this yields a much smaller voltage to reach similar injection concentrations, the limiting factor is still the breakdown field, not the voltage, which is independent of the dielectric thickness. Moreover, the spectral tuning demonstrated here is also comparable to other reported values of electrical tuning of the plasmonic resonances using active materials such as graphene.[12,13]

In summary, we demonstrated an electrically tunable plasmonic "perfect" absorber. The "gold nanostrip antenna/dielectric spacer/gold back plate" structure forms a plasmonic resonator with unity absorption. Electrical tuning of the absorption spectrum is realized by the modulated refractive index of a thin ITO layer strongly coupled to the plasmonic absorber near field.

This work was supported partially by the MRSEC Program of NSF under Award No. DMR11-20901 and Penn URF. Parts of this work were carried out in the University of Pennsylvania Nanofabrication Facility, Nano/Bio Interface Center (NBIC), which receives partial support from NSF and the Penn Regional Nanotechnology Facility (PRNF), which is a member of the NSF-funded Materials Research Facilities Network via the MRSEC program. We gratefully acknowledge expert help from Dr. Humeyra Caglayan for optical characterization of ITO films.

[1]E. Cubukcu, N. F. Yu, E. J. Smythe, L. Diehl, K. B. Crozier, and F. Capasso, IEEE J. Sel. Top. Quantum Electron. **14**(6), 1448 (2008).
[2]H. Zhu, F. Yi, and E. Cubukcu, IEEE Photonics Technol. Lett. **24**(14), 1194 (2012).
[3]C. Wu, B. Neuner III, G. Shvets, J. John, A. Milder, B. Zollars, and S. Savoy, Phys. Rev. B **84**(7), 075102 (2011).
[4]X. L. Liu, T. Starr, A. F. Starr, and W. J. Padilla, Phys. Rev. Lett. **104**(20), 207403 (2010).
[5]A. Melikyan, N. Lindenmann, S. Walheim, P. M. Leufke, S. Ulrich, J. Ye, P. Vincze, H. Hahn, T. Schimmel, and C. Koos, Opt. Express **19**(9), 8855 (2011).
[6]E. Feigenbaum, K. Diest, and H. A. Atwater, Nano Lett. **10**(6), 2111 (2010).
[7]V. J. Sorger, N. D. Lanzillotti-Kimura, R. M. Ma, and X. Zhang, Nanophotonics **1**(1), 17 (2012).
[8]W. W. Salisbury, U.S. patent 2,599,944 (1952).
[9]R. M. Tiggelaar, A. W. Groenland, R. G. P. Sanders, and J. G. E. Gardeniers, J. Appl. Phys. **105**(3), 033714 (2009).
[10]S. M. Sze and K. K. Ng, *Physics of Semiconductor Devices* (Wiley-Interscience, 2006).
[11]X. Wang, D. Vasileska, and G. Klimeck (2010), "ABACUS - Assembly of Basic Applications for Coordinated Understanding of Semiconductors," https://nanohub.org/resources/abacus. (DOI:10.4231/D3XW47W0J) .
[12]N. K. Emani, T. F. Chung, X. J. Ni, A. V. Kildishev, Y. P. Chen, and A. Boltasseva, Nano Lett. **12**(10), 5202 (2012).
[13]Y. Yao, M. A. Kats, P. Genevet, N. F. Yu, Y. Song, J. Kong, and F. Capasso, Nano Lett. **13**(3), 1257 (2013).